Int. J. Electrochem. Sci., 12 **(2017)** 9161 – 9179, doi: 10.20964/2017.10.51

International Journal of ELECTROCHEMICAL SCIENCE
www.electrochemsci.org

Effects of Pre-Corrosion on the Corrosion Inhibition Performance of Three Inhibitors on Q235 Steel in CO_2/H_2S Saturated Brine Solution

Chen Zhang[1], *Jingmao Zhao*[1,2,*]

[1] College of Material Science and Engineering, Beijing University of Chemical Technology, Beijing 100029, China
[2] Beijing Key Laboratory of Electrochemical Process and Technology for Materials, Beijing 100029, China
[*]E-mail: jingmaozhao@126.com

Received: 8 June 2017 / *Accepted:* 7 August 2017 / *Published:* 12 September 2017

Effects of pre-corrosion on the corrosion inhibition performance of three inhibitors on Q235 steel in a CO_2/H_2S saturated brine solution were investigated with potentiodynamic polarization, electrochemical impedance spectroscopy (EIS), scanning electron microscope (SEM), X-ray diffraction (XRD), energy dispersive spectrometer (EDS), and X-ray photoelectron spectroscopy (XPS). The results showed that the corrosion rate of steels was decreased significantly after pre-corrosion for different times indicating a good protection effect of the pre-corrosion products, which were composed of mostly FeS and limited $FeCO_3$. The inhibitors could both inhibit the CO_2/H_2S corrosion of freshly abraded Q235 steels and the pre-corroded ones, but the pre-corrosion could gradually deteriorate their inhibition performances with the increase of pre-corrosion time. And the difference in their inhibition performances became relative distinct after pre-corrosion for 7 days possibly due to the differences of their molecular structures. According to the XPS results, the inhibitor films could be formed on the surface of the corrosion product layer. However, the corrosion species might be also diffused to the steel surface through the diffusion channels in the corrosion products and attack the steel matrix.

Keywords: Tetradecyl trimethyl ammonium bromide; N-benzyl pyridinium chloride; Imidazoline quaternary ammonium salt; Pre-corrosion; Acid corrosion

1. INTRODUCTION

The corrosion of CO_2 and H_2S mixture is a severe form of attack on steel in the production and transportation of oil and gas [1-3]. In petroleum industry, many methods have been used to inhibit

CO_2/H_2S corrosion, and the injection of organic corrosion inhibitor is one of the most cost-effective methods.

Organic corrosion inhibitors can effectively retard the corrosion of steel through forming a compact barrier film between steel surface and corrosive medium [4-7]. Most organic corrosion inhibitors contain heteroatoms, such as nitrogen, oxygen, phosphorus and sulphur as well as triple bond or aromatic ring, considered as the reaction center for the adsorption process [8-10] because the heteroatoms can donate their lone electron pairs to the empty d-orbitals of Fe atoms to form the coordinate covalent bonds [11, 12]. Moreover, in some cases, the electrostatic interaction between inhibitor molecules and steel surface is also favorable for the adsorption of inhibitors [13-15].

Although many high-efficiency corrosion inhibitors were reported in various corrosive environments, most of the studies were carried on freshly abraded samples. However, in practical applications, the pipelines may have been went into service for a long time and covered by a corrosion product layer, such as iron carbonate and iron sulfide, before adding inhibitors. These corrosion products may influence the corrosion inhibition performance of inhibitors. The effect of pre-corrosion on the corrosion inhibition performance of inhibitors in CO_2 brine solution was reported [16, 17]. The results showed that the pre-corrosion deteriorated the inhibition performance because of the presence of laminar cementite. The inhibition performance of an imidazoline-based inhibitor in a CO_2-saturated brine solution was evaluated [18], and the results indicated that pre-corrosion had a detrimental effect on the performance of inhibitor due to the residual cementite and element Cu and the formation of $FeCO_3$ on the surface of pre-corroded sample. The negative effect of pre-corrosion on the performance of inhibitors was also discovered by some other scholars [19, 20]. On some cases, after the pre-corrosion, the performances of inhibitors was not be affected significantly [21, 22]. However, the enhancement of the corrosion inhibition performance of C16 quaternary amine by pre-corrosion in the CO_2 brine solution has been reported [23], which is due to the more rapid alterations in the structure of $FeCO_3$ caused by the inhibitor on a pre-corroded surface than on an initially clean one. Therefore, the effect of pre-corrosion is still not very clear on the inhibition performance of inhibitors, especially, in the CO_2/H_2S brine solution.

In this study, the influence of pre-corrosion on the corrosion inhibition performance of tetradecyl trimethyl ammonium bromide, *N*-benzyl pyridinium chloride and imidazoline quaternary ammonium salt on carbon steel in a CO_2/H_2S saturated brine solution was investigated with potentiodynamic polarization and electrochemical impedance spectroscopy. The surface features of samples pre-corroded for different time were studied with scanning electron microscope and X-ray diffraction. The inhibitors adsorbed on the surface of the pre-corroded carbon steel were detected with X-ray photoelectron spectroscopy.

2. EXPERIMENTAL METHOD

2.1 Materials

Q235 steel is composed of 0.19 wt.% C, 0.59 wt.% Mn, 0.3 wt.% Si, 0.044 wt.% P, 0.05 wt.% S and bal. Fe. The samples was cut into coupons with the size of 10×10×3 mm for electrochemical measurements and surface features analysis, and 5×5×2 mm for X-ray photoelectron spectroscopy analysis. Before its usage, coupons were abraded by emery paper (up to 2000 grit), rinsed with ethanol and dried in air.

Analytical grade tetradecyl trimethyl ammonium bromide (TTAB) was used as inhibitor. *N*-benzyl pyridinium chloride (BPC, 95 %) and imidazoline quaternary ammonium salt (IAS, 95 %) were obtained from LFHX Co. Ltd., China. Their molecular structures are shown in Fig. 1.

The brine solution, 3.5 wt.% NaCl solution, was prepared from analytical grade NaCl and distilled water. Before Q235 steel coupons were immersed into the brine solution, a mixture of H_2S (80 ml min^{-1}) and CO_2 (80 ml min^{-1}) was introduced into the solution for 4 h to make a CO_2/H_2S-saturated brine solution. The pre-corroded samples were prepared after coupons were immersed into the CO_2/H_2S-saturated brine solution for different times, then taken out from the solution and dried in air. Samples were stored in a desiccator to prevent oxidizing.

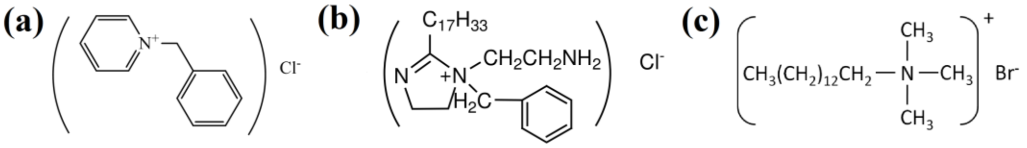

Figure 1. Molecular structures of (a) BPC, (b) IAS and (c) TTAB.

2.2 Electrochemical measurements

The electrochemical measurements were performed in a conventional three-electrode cell with a Gamry interface 1000 electrochemical workstation at 60±1 °C. The cell was filled with 200 mL of CO_2/H_2S-saturated brine solution, and the saturated calomel electrode (SCE) and platinum electrode were selected as the reference electrode and the counter electrode, respectively. Prior to each electrochemical experiment, the work electrode was immersed into the solution for 2 h to reach a stable state (the fluctuation of open circuit potential (OCP) is less than ±5 mV vs. SCE). Each electrochemical measurement was repeated for three times to ensure a good reproducibility.

In the potentiodynamic polarization experiments, the potential changed from -200 to +200 mV vs. OCP at a scan rate of 0.16 mVs^{-1}. The electrochemical parameters can be obtained through fitting polarization curves with software Cview. Subsequently, the inhibition efficiency, η_p, can be evaluated from the corrosion current density (i_{corr}) as the following,

$$\eta_p = \frac{i_{corr} - i_{corr(inh)}}{i_{corr}} \times 100\% \qquad (1)$$

where i_{corr} and $i_{corr(inh)}$ are the corrosion current densities without and with inhibitor, respectively.

In EIS test, the frequency was changed from 100 kHz to 0.01 Hz with the perturbation amplitude of 5 mV vs. OCP. The electrochemical parameters can be obtained through fitting impedance data with software Zsimpwin. Subsequently, the inhibition efficiency, η_Z, can be estimated from the calculated R_t with the following equation,

$$\eta_Z = \frac{R_{t(inh)} - R_t}{R_{t(\mathrm{int})}} \times 100\% \qquad (2)$$

where R_t and $R_{t(inh)}$ are the total resistances without and with inhibitor, respectively.

2.3 Surface analysis

A scanning electron microscope (SEM, FEI Quanta 200 F field) equipped with energy dispersive spectroscopy (EDS) was used to study the surface feature of the pre-corroded samples. The corrosion products on the samples were characterized with an X-ray diffraction (XRD, Bruker D8 Focus). The XPS analysis was performed on the samples covered with inhibitor films with a PHI-5300ESCA spectrometer (Perkin–Elmer, USA). The existent elements on steel surface were obtained from wide-scan XPS spectra, and the chemical states of these elements were obtained from the high-resolution spectra. In this study, the binding energy of C1s at 284.6 eV was used to calibrate other binding energies. The fitting of XPS data was carried on with software XPSPEAK.

3. RESULTS AND DISCUSSION

3.1. Potentiodynamic polarization measurement

Potentiodynamic polarization curves were measured on the freshly abraded electrodes and the electrodes pre-corroded for 4 hours, 1 day, 3 days, 5 days and 7days in the CO_2/H_2S-saturated brine solution at 60±1 °C to evaluate the effect of pre-corrosion on the corrosion inhibition performance of inhibitors. By fitting the polarization curves, the electrochemical parameters were obtained (Table 1). Inhibitors, IAS, TTAB and BPC, exhibited good corrosion inhibition performance on the freshly abraded Q235 steel in the CO_2/H_2S-saturated brine solution, and these three compounds apparently belonged to anodic-type inhibitors because their displacements in corrosion potential (E_{corr}) were all above 85 mV [24, 25].

When the samples were covered by corrosion products, the i_{corr} without inhibitors in the solution was decreased with the increase of the pre-corrosion time, indicating that the formation of corrosion products could retard the corrosion of steel to some extent. After inhibitors were added in the solution, the η_p values of TTAB, BPC and IAS all were decreased with the increase of the pre-corrosion time, indicating a negative effect of pre-corrosion on the corrosion inhibition performance of these three inhibitors. Additionally, similar inhibition performances of TTAB, BPC and IAS were observed on the freshly abraded electrodes and the electrodes pre-corroded for short time. While, a relatively distinct difference in their inhibition performance appeared after pre-corrosion for 7 days possibly due to the differences in their molecular structures.

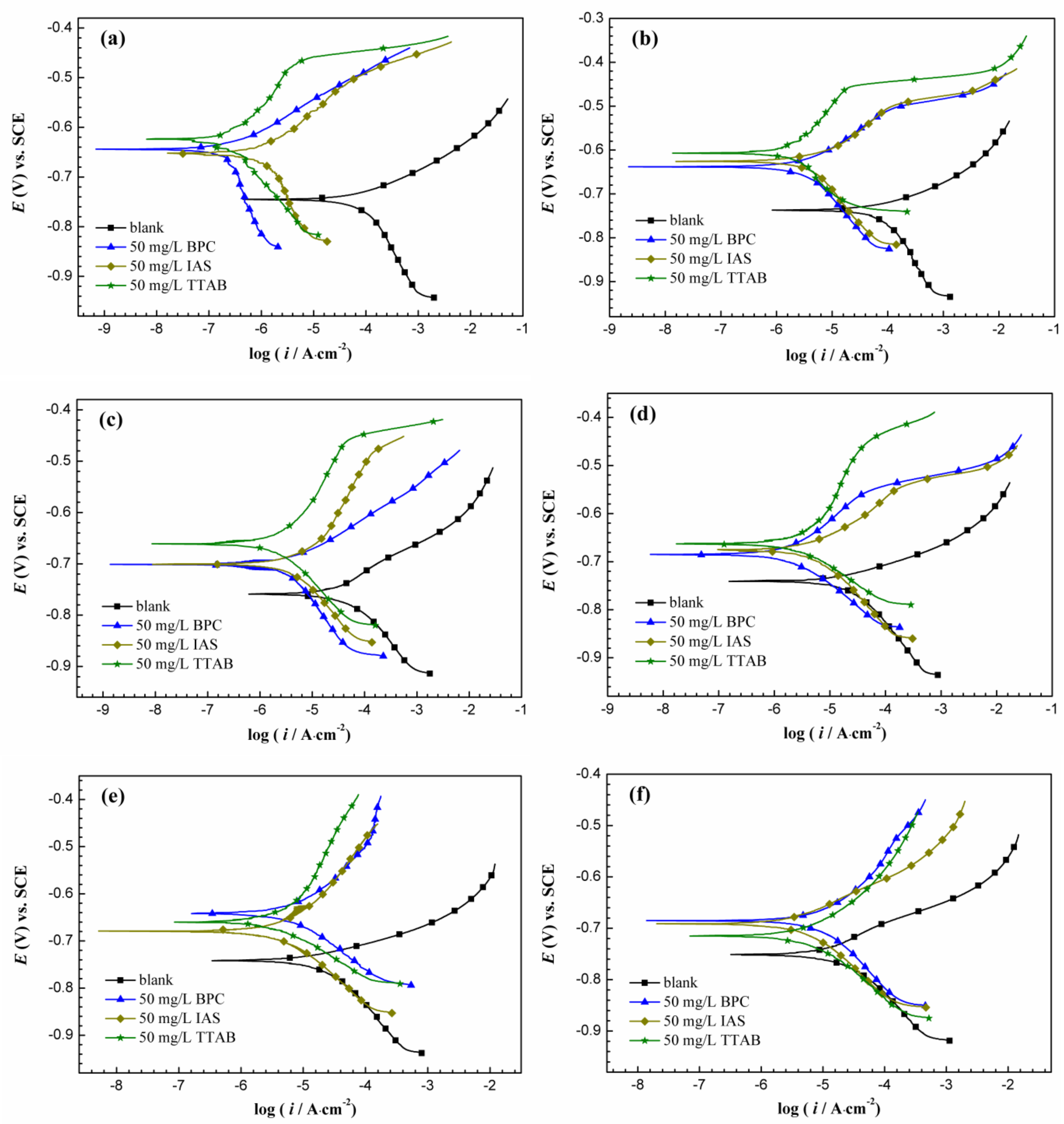

Figure 2. Polarization curves measured on the (a) freshly abraded samples and samples pre-corroded for (b) 4 hours, (c) 1 day, (d) 3 days, (e) 5 days, and (f) 7 days in the CO_2/H_2S-saturated brine solution with different inhibitors at 60 ˚C.

Table 1. Electrochemical parameters from the fitted polarization curves of freshly abraded and pre-corroded samples in the CO_2/H_2S-saturated brine solution with different inhibitors at 60 ˚C

Pre-corrosion time	Inhibitor (mg/L)	βa (mV/dec)	βc (mV/dec)	E_{corr} vs.SCE (mV)	i_{corr} (μA/cm^2)	η_p (%)
Without pre-corrosion	blank	56.75	-196.43	-746.00	90.1	-
	50 mg/L BPC	56.23	-202.85	-644.13	0.25	99.7
	50 mg/L IAS	68.05	-124.71	-652.38	0.49	99.5

	50 mg/L TTAB	115.83	-71.02	-624.00	0.35	99.6
4 hours	blank	56.47	-199.81	-737.00	81.4	-
	50 mg/L BPC	73.56	-109.66	-638.06	2.97	96.4
	50 mg/L IAS	56.75	-196.42	-626.00	4.40	94.6
	50 mg/L TTAB	79.43	-98.77	-608.00	2.13	97.4
1 day	blank	65.80	-133.05	-758.63	43.4	-
	50 mg/L BPC	63.51	-143.54	-701.06	3.60	91.7
	50 mg/L IAS	76.81	-103.15	-701.00	4.45	89.7
	50 mg/L TTAB	63.96	-141.27	-661.25	1.57	96.4
3 days	blank	50.32	-351.89	-743.62	28.1	-
	50 mg/L BPC	92.43	-84.08	-684.87	3.66	87.0
	50 mg/L IAS	75.06	-106.48	-676.00	3.46	87.7
	50 mg/L TTAB	113.87	-71.78	-662.62	2.68	90.5
5 days	blank	51.2	-314.4	-742.00	22.8	-
	50 mg/L BPC	93.12	-83.51	-642.00	6.20	72.8
	50 mg/L IAS	106.69	-74.96	-679.38	3.71	83.7
	50 mg/L TTAB	119.33	-69.77	-659.63	3.65	84.0
7 days	blank	60.35	-162.78	-751.31	19.7	-
	50 mg/L BPC	83.28	-93.41	-686.00	8.10	58.9
	50 mg/L IAS	66.08	-131.91	-691.25	4.93	75.0
	50 mg/L TTAB	87.12	-89.00	-715.00	6.00	69.5

3.2 Electrochemical impedance spectroscopy measurements

The Nyquist and Bode plots were measured to further verify the negative effect of pre-corrosion on the corrosion inhibition performance of TTAB, BPC and IAS. As shown in Fig. 3(a1~d1), with the increase of pre-corrosion time, the diameters of the capacitive loop of TTAB, BPC and IAS were all decreased gradually indicating the deterioration of their corrosion inhibition performance.

As shown in Fig. 3(a2~d2), most Bode plots only had one peak indicating that these systems could be described with one-time constant model (Fig. 4(a), where, R_s is the solution resistance, R_{ct} represents the charge transfer resistance, and Q_{dl} is the constant phase element which is used to replace the double-layer capacitor (C_{dl}) in order to give a more accurate fit [26]).

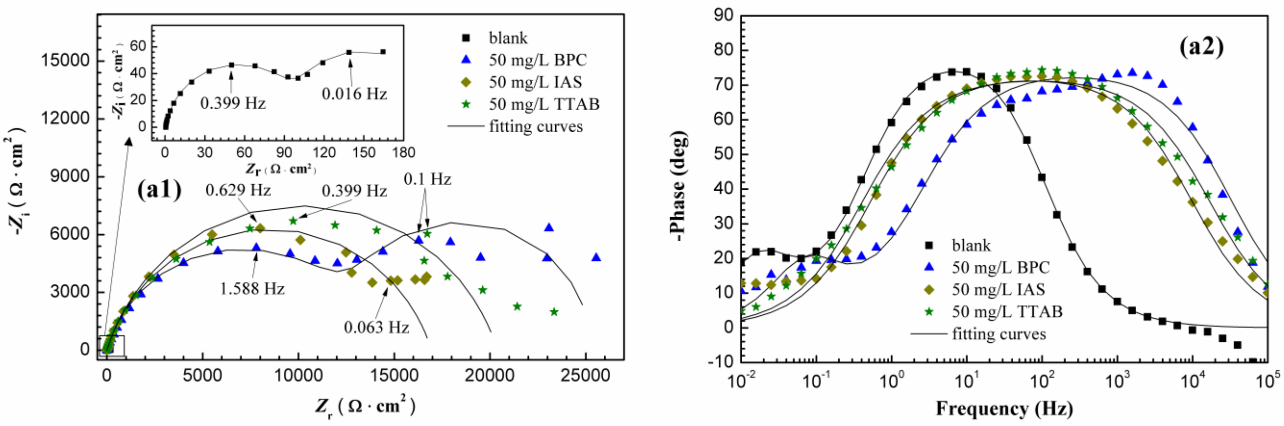

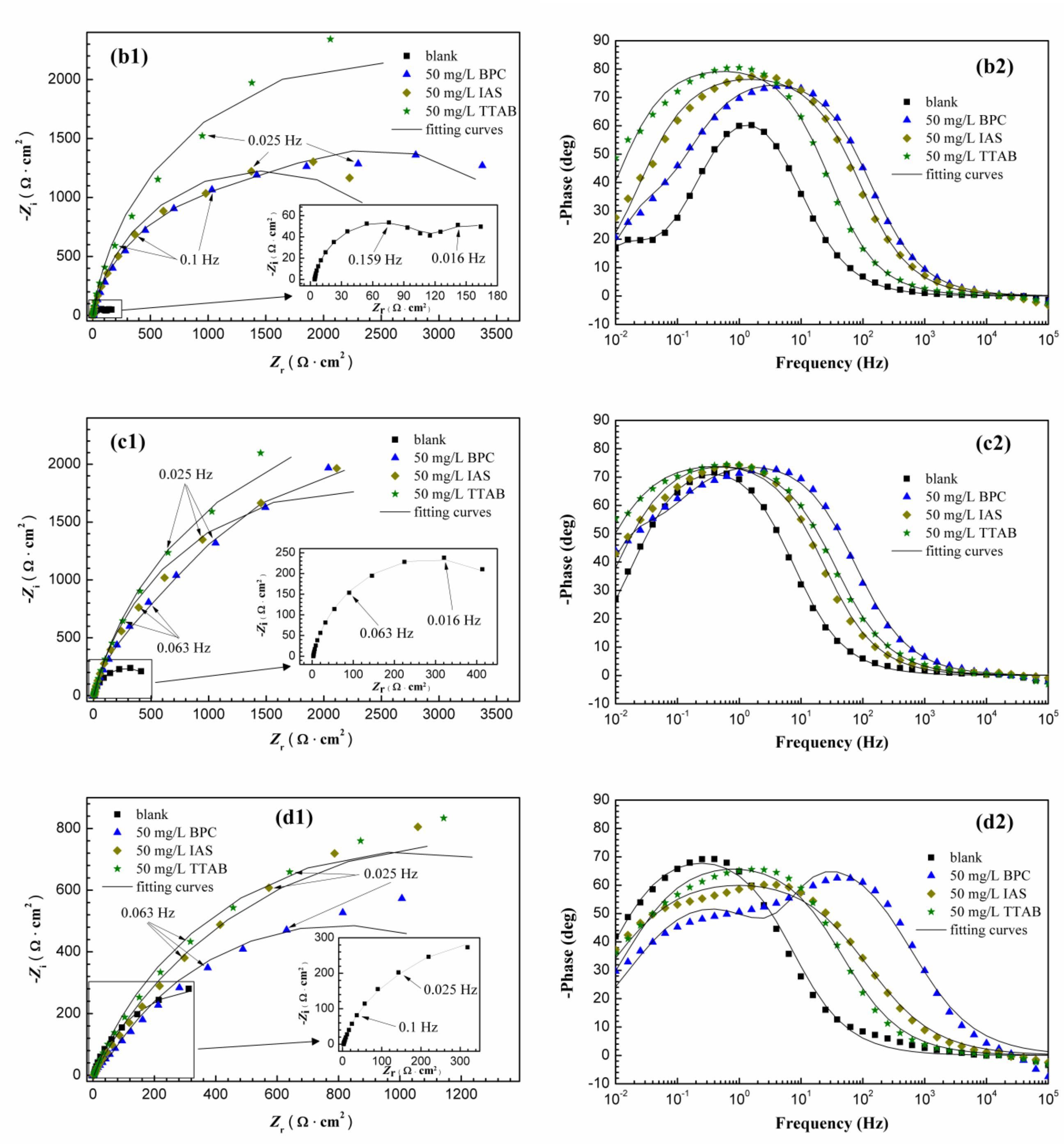

Figure 3. Nyquist and Bode plots measured on the (a1, a2) freshly abraded samples and samples pre-corroded for (b1, b2) 4 hours, (c1, c2) 3 days, and (d1, d2) 7 days in the CO_2/H_2S-saturated brine solution with different inhibitors at 60 °C.

However, some experimental data should be fitted with the equivalent circuit in Fig. 5(b), which contained the resistance of inhibitor film (R_f) or corrosion product film (R_{cp}) and the capacitance of inhibitor film (C_f) or corrosion product film (C_{cp}).

The electrochemical parameters were obtained from the fitted impendence data and listed in Table 2. The total resistance (R_t) of the system was the sum of R_{ct} and R_f or R_{cp}, and used to calculate the η_z [27]. According to the variation of η_z values vs pre-corrosion time, the pre-corrosion deteriorated the corrosion inhibition performance of TTAB, BPC and IAS. These results obtained from EIS and polarization measurements were in good agreement.

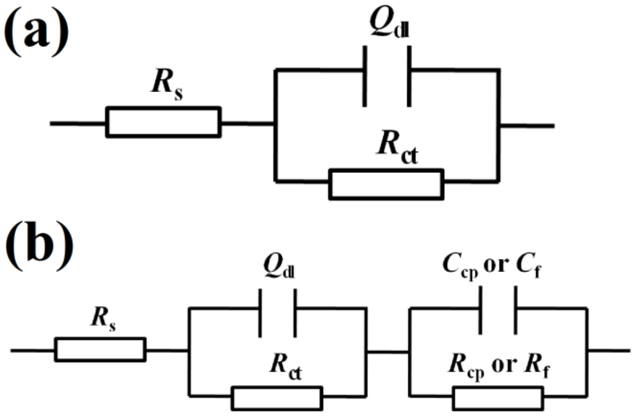

Figure 4. Electrochemical equivalent circuit used to fit the impedance spectra measured on the freshly abraded and pre-corroded samples in the CO_2/H_2S-saturated brine solution with different inhibitors at 60 ˚C.

Table 2. Electrochemical parameters from the EIS data of freshly abraded and pre-corroded samples in the CO_2/H_2S-saturated brine solution with different inhibitors at 60 ˚C

			Q_{dl}					
Pre-corrosion time	Inhibitor (mg/L)	R_s ($\Omega\cdot cm^2$)	Y ($\mu\Omega^{-1}\cdot cm^{-2}\cdot S^n$)	n	R_{ct} ($\Omega\cdot cm^2$)	C_{cp} or C_f ($F\cdot cm^{-2}$)	R_{cp} or R_f ($\Omega\cdot cm^2$)	η_z (%)
Without pre-corrosion	blank	4.602	4222	0.9147	105.6	0.1221	99.6	-
	50 mg/L BPC	5.140	8.361	0.8232	1.311×10^4	2.463×10^{-4}	1.217×10^4	99.2
	50 mg/L IAS	5.752	22.19	0.8131	1.693×10^4	-	-	98.8
	50 mg/L TTAB	3.821	22.93	0.8069	2.039×10^4	-	-	99.0
4 hours	blank	4.244	6789	0.8875	117.1	0.1921	85.9	-
	50 mg/L BPC	4.219	731.3	0.8672	2210	4.277×10^{-3}	1740	94.9
	50 mg/L IAS	2.136	1757	0.8820	2951	-	-	93.1
	50 mg/L TTAB	3.469	2477	0.9127	4910	-	-	95.9
3 days	blank	3.013	11330	0.8778	570.0	-	-	-
	50 mg/L BPC	2.708	2446	0.8305	3697	5.632×10^{-3}	896	87.5
	50 mg/L IAS	2.798	2389	0.8609	4393	-	-	87.0
	50 mg/L TTAB	3.247	3085	0.8480	5933	-	-	90.4
7 days	blank	2.684	15940	0.8253	729.5	-	-	-
	50 mg/L BPC	1.058	3017	0.7071	1566	1.027×10^{-3}	24.8	54.1
	50 mg/L IAS	2.813	3366	0.7038	2426	-	-	69.9
	50 mg/L TTAB	3.713	3217	0.7792	2066	-	-	64.7

3.3 Surface feature analysis

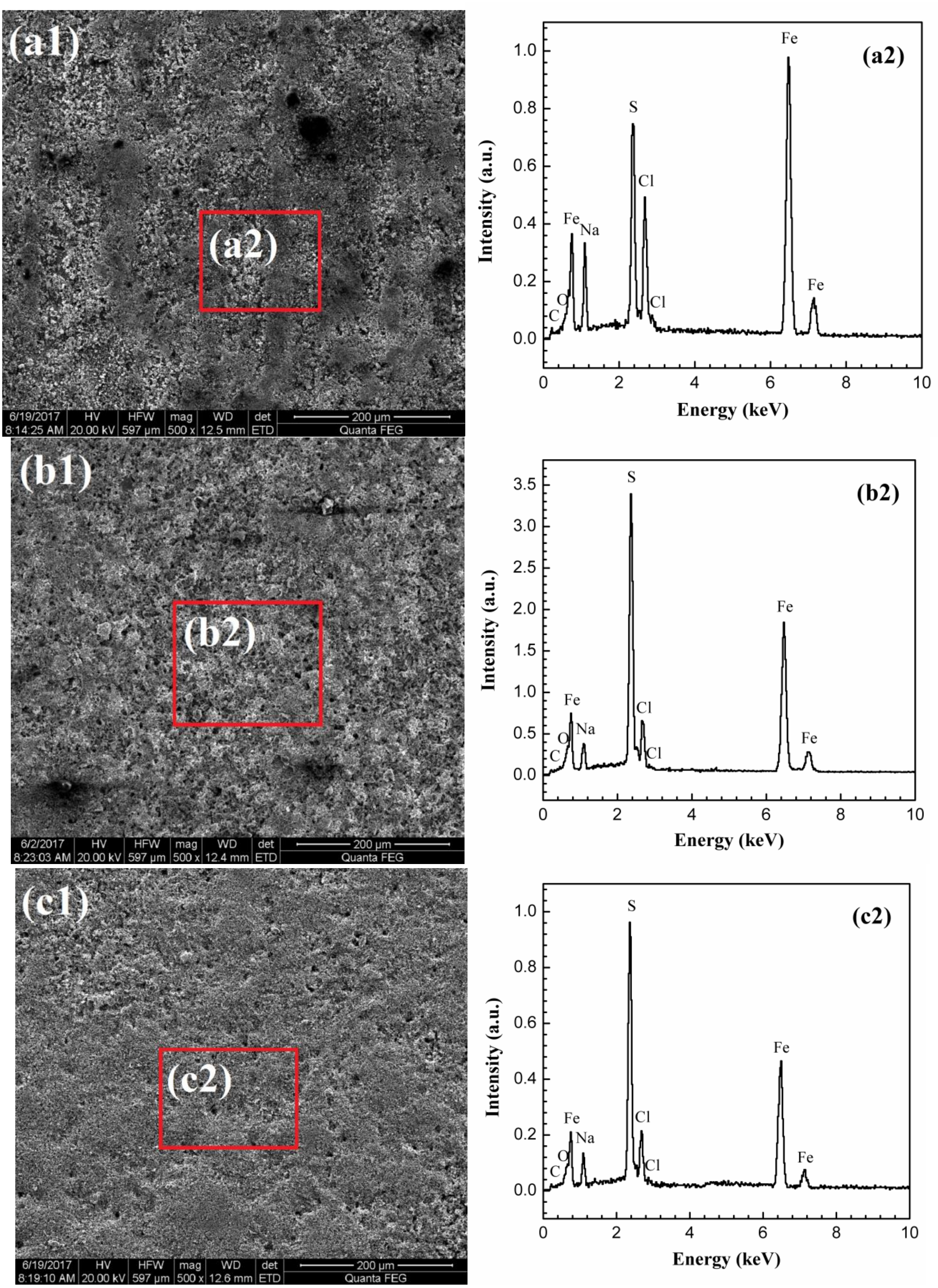

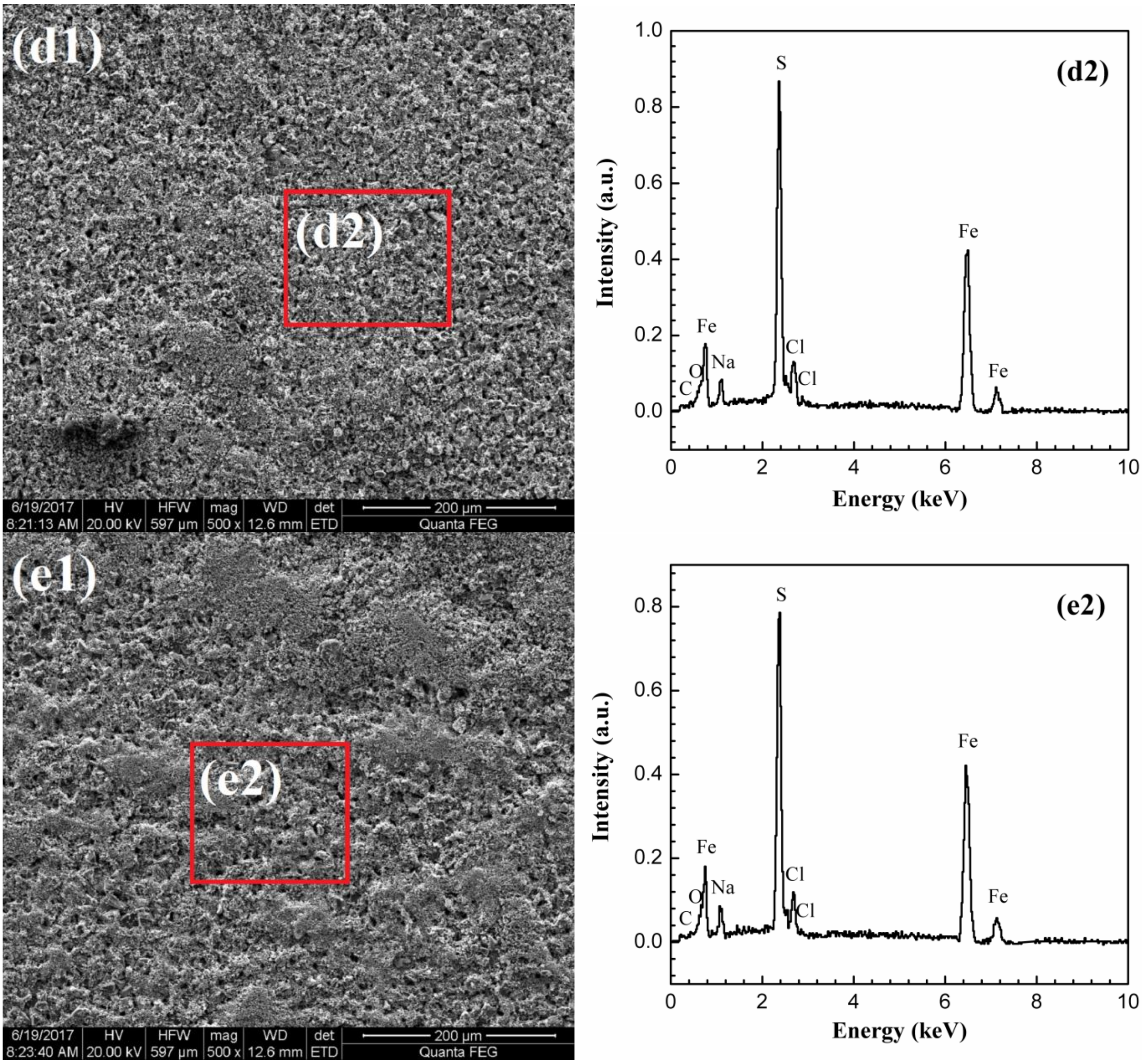

Figure 5. SEM images and EDS results of samples pre-corroded for (a1, a2) 4 hours, (b1, b2) 1 day, (c1, c2) 3 days, (d1, d2) 5 days and (e1, e2) 7 days in the CO_2/H_2S-saturated brine solution without inhibitors at 60 °C.

Fig. 5 shows the surface morphologies and corresponding EDS results of the samples pre-corroded for 4 hours, 1 day, 3 days, 5 days and 7 days in the CO_2/H_2S-saturated brine solution without inhibitors at 60 °C, and Table 3 lists the relevant atomic percentage of Fe, C, O and S. With the increase of pre-corrosion time, the atomic percentages of C and O had no significant change, and the atomic percentages of S and Fe was remarkably increased and decreased, respectively, initially, and then almost remained unchanged.

According to XRD results (Fig. 6), the corrosion products mainly consisted of $FeCO_3$ and FeS, and the amount of FeS was much higher than that of $FeCO_3$. Additionally, with the increase of pre-corrosion time, the significant decrease of Fe and increase of FeS happened simultaneously, and the surface of pre-corroded sample with relative long pre-corrosion time (5 days or 7 days) was almost covered by corrosion products mainly containing FeS.

Fig. 7 shows the cross section of samples pre-corroded for 4 hours, 3 day and 7 days. As shown in Fig. 7(a), few corrosion products were on the steel surface. When the pre-corrosion time was increased to 3 days (Fig. 7(b)), the corrosion product film could be easily detected. And the thickness of this film was continuously increased with the increase of pre-corrosion time (Fig. 7(c)).

Table 3. Atomic percentage for Fe, C, O and S measured with EDS on the samples pre-corroded for 4 hours, 1 day, 3 days, 5 days and 7 days in the CO_2/H_2S-saturated brine solution without inhibitors at 60 ˚C

Element	Pre-corrosion time				
	4 hours	1 day	3 days	5 days	7 days
C	8.16	10.74	12.94	11.78	11.89
O	7.05	6.40	7.05	6.94	6.49
S	22.42	38.08	37.93	36.85	36.43
Fe	62.38	44.79	42.09	44.43	45.19

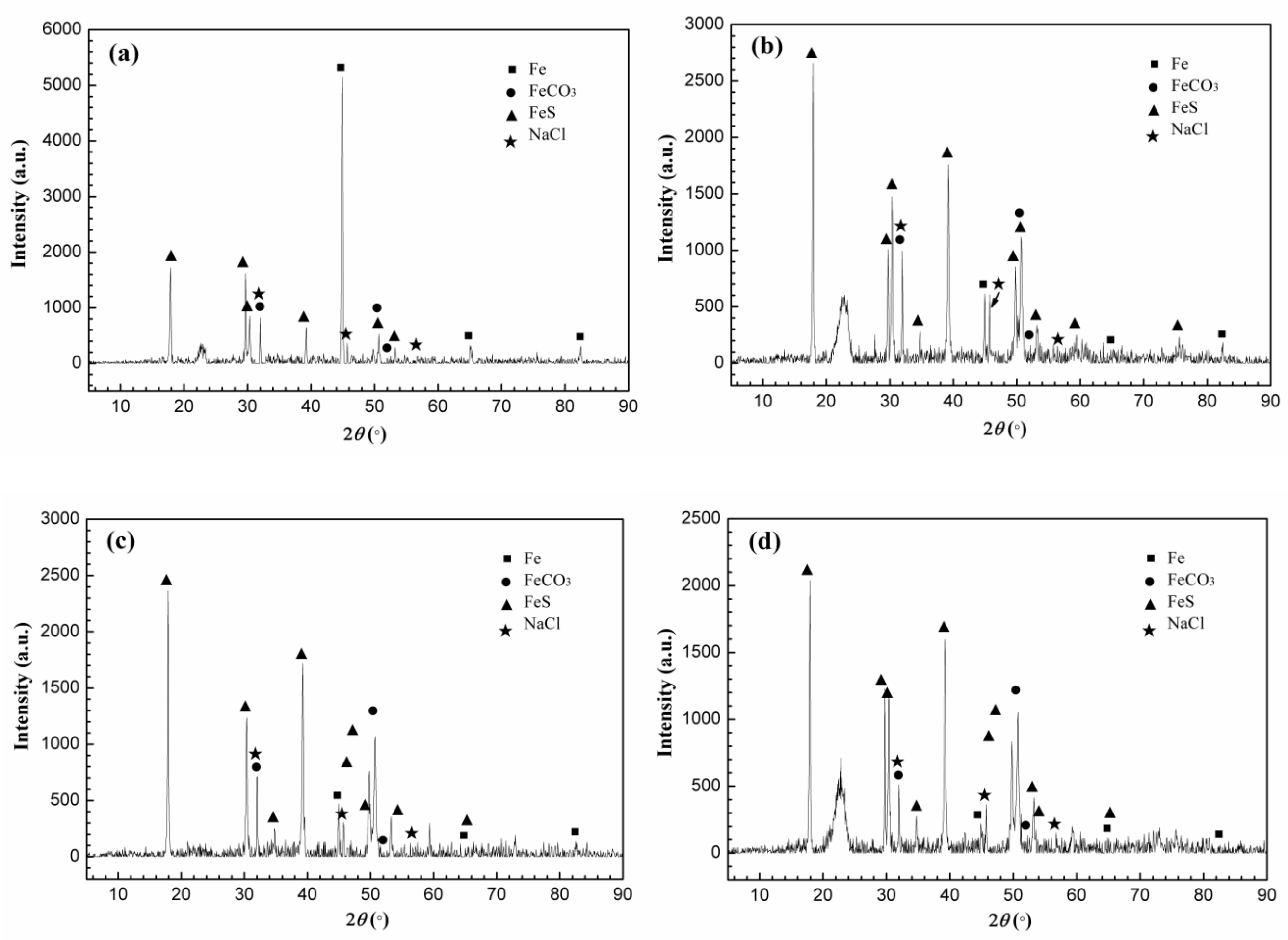

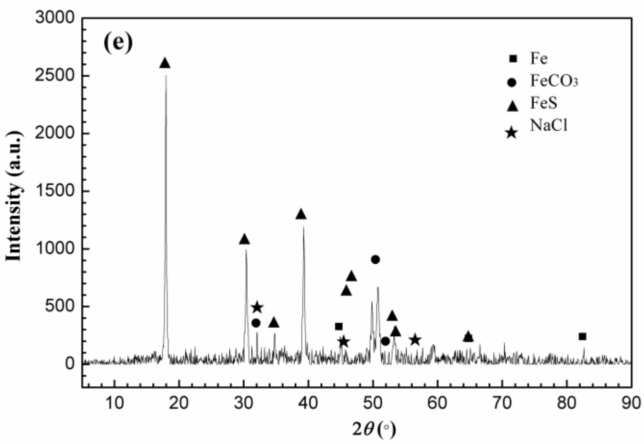

Figure 6. XRD results of samples pre-corroded for (a) 4 hours, (b) 1 day, (c) 3 days, (d) 5 days and (e) 7 days in the CO_2/H_2S-saturated brine solution without inhibitors at 60 °C.

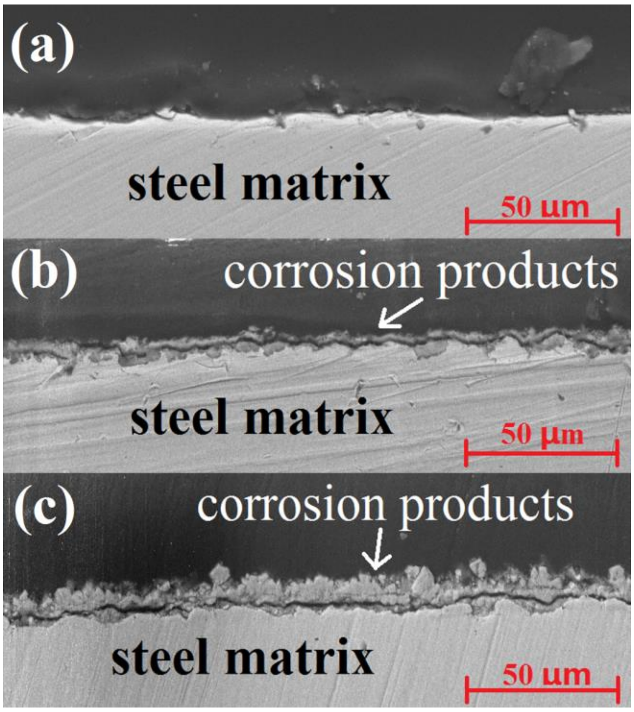

Figure 7. Cross section micrograph of the samples pre-corroded for (a) 4 hours, (b) 3 days and (c) 7 days in the CO_2/H_2S-saturated brine solution without inhibitors at 60 °C.

3.4 X-ray photoelectron spectroscopy (XPS) analysis

The coupons were first immersed in the CO_2/H_2S saturated-brine solution without inhibitors for 3 days at 60 °C, and then the pre-corroded samples were immersed in the corrosive solution with different inhibitors for 4 h. The XPS analyses were performed on the samples covered with inhibitor films. Fig. 8 shows the wide-scan spectra of the pre-corroded samples. The peaks of Na_{1s}, Fe_{2p}, O_{1s}, N_{1s}, C_{1s}, Cl_{2s}, Cl_{2p} and S_{2p} could be found in the spectra. Elements Na and Cl were due to the residual sodium chloride; the signals of C_{1s} and N_{1s} were mainly attributed to the inhibitors absorbed on the steel surface; the signals of S_{2p} and O_{1s} came from the corrosive products; and the signal of Fe_{2p} could be assigned to the iron matrix and its corrosion products.

The high-resolution spectra of C_{1s} were shown in Fig. 9. The spectra in Fig. 9(a) and (b) could both be decomposed into three peaks, which were attributed to the C atoms in alkyl group (CH_x) at 284.6 eV [28], –C= and –C–N at 285.8 eV [28-30], and –C=N at 288.0 eV [30]. Two peaks could be found in Fig. 9(c), which were due to CH_x at 284.6 eV [28] and –C–N at 285.8 eV [28, 30].

Fig. 10 shows the high-resolution spectra of N_{1s}. Two peaks could be found both in Fig. 10(a) and (b). Peaks at 401.8 eV and 401.4 eV are assigned to the positively charged nitrogen [30]. Peaks at 399.8 eV and 400.2 eV were due to the –N= of the incompletely reacted pyridine, and the –N= and –NH_2 in IAS, respectively [30, 31]. In Fig. 10(c), the only peak at 402.3 eV could be attributed to the –$N^+(CH_3)_3$ in TTAB [32, 33].

Two peaks at 161.7 eV and 167.5±0.1 eV could be obviously observed in the high-resolution spectra of S_{2p} (Fig. 11), which could be attributed to the ferrous sulfide on steel surface [34, 35] and the oxidation of sulfur [35, 36].

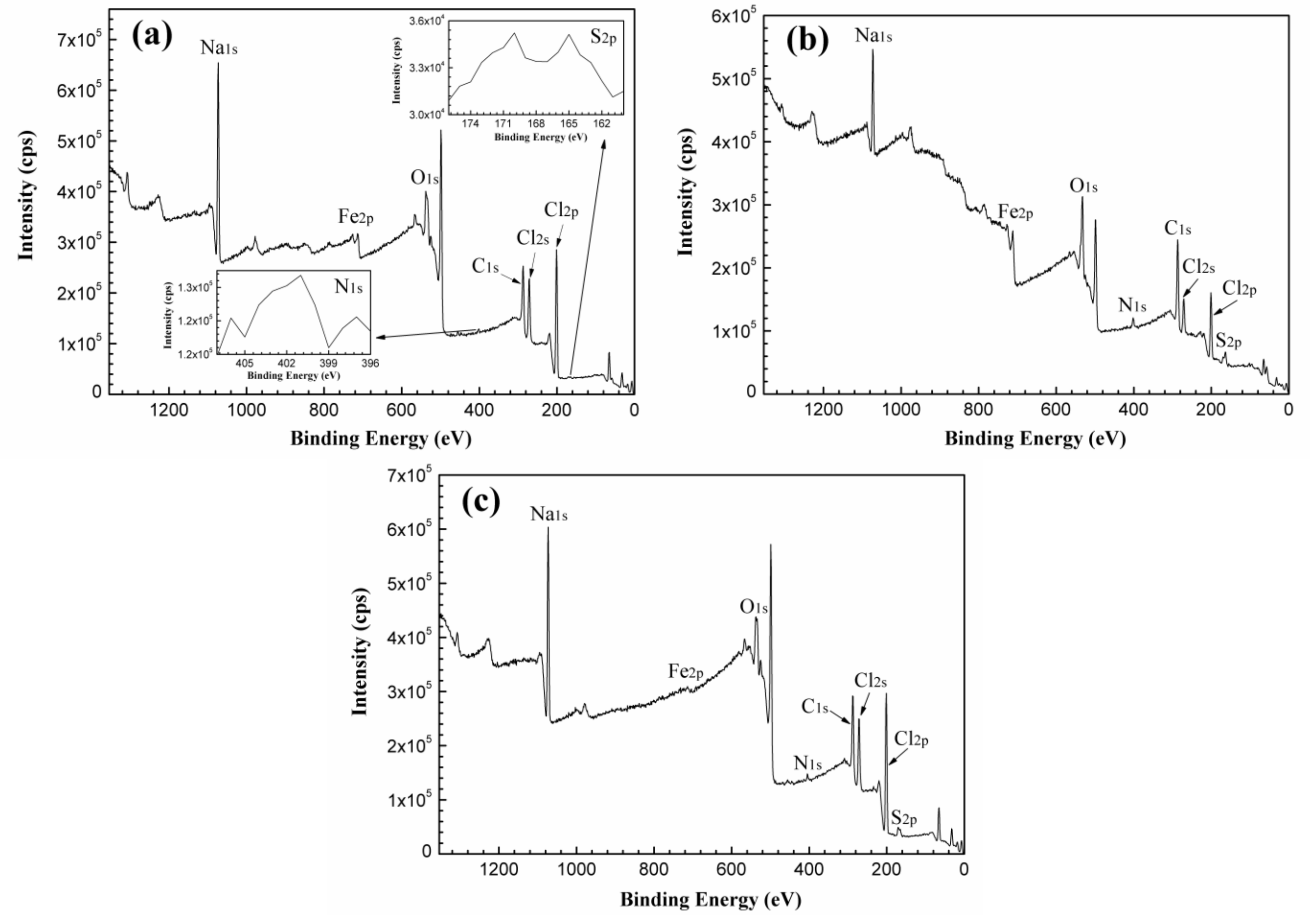

Figure 8. Wide-scan XPS spectra of Q235 steels pre-corroded for 3 days after the immersion in the CO_2/H_2S-saturated brine solution with (a) 50 mg L^{-1} BPC, (b) 50 mg L^{-1} IAS, and (c) 50 mg L^{-1} TTAB for 4 h at 60 °C.

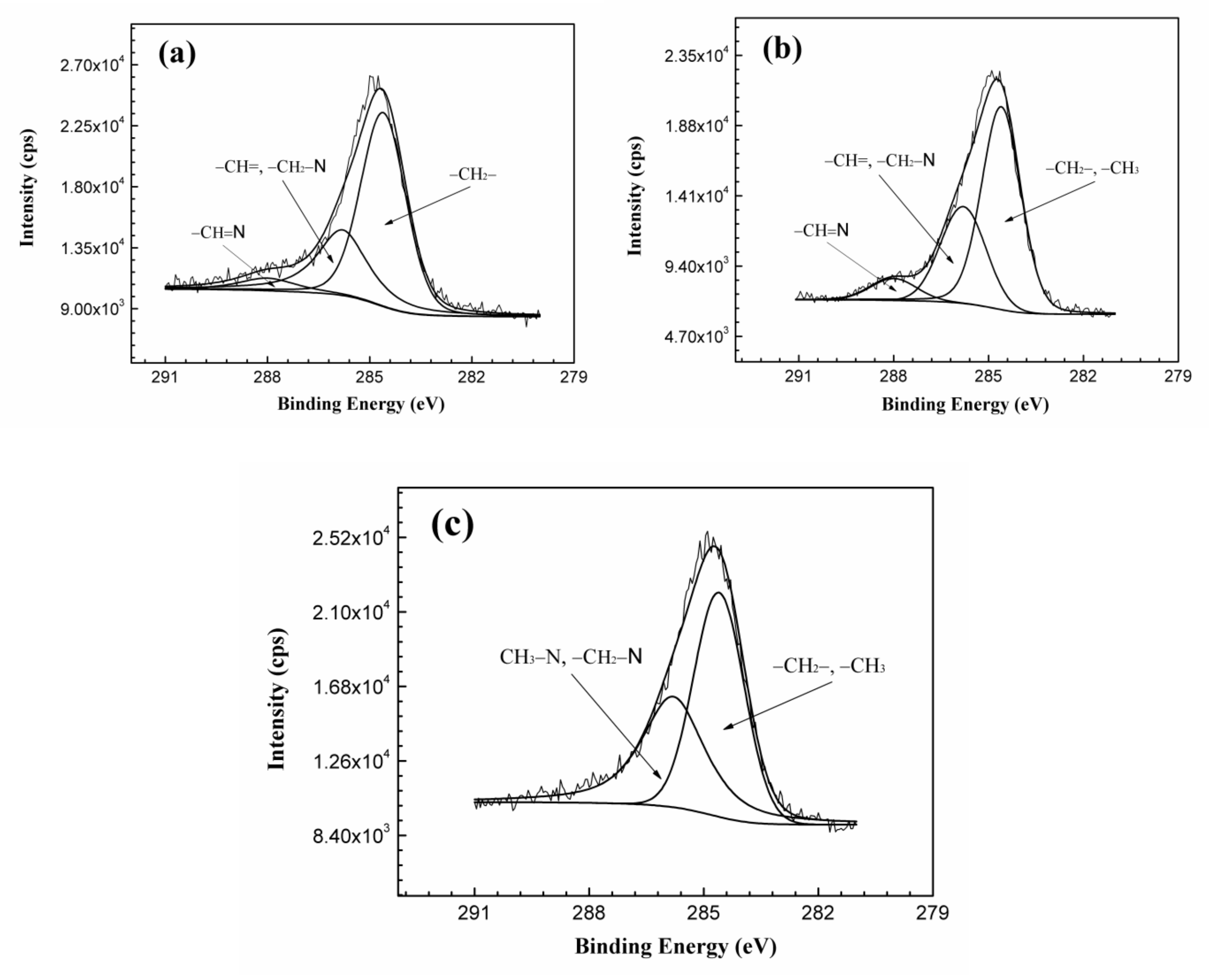

Figure 9. High-resolution XPS spectra of C_{1s} of Q235 steels pre-corroded for 3 days after the immersion in the CO_2/H_2S-saturated brine solution with (a) 50 mg L^{-1} BPC, (b) 50 mg L^{-1} IAS, and (c) 50 mg L^{-1} TTAB for 4 h at 60 °C.

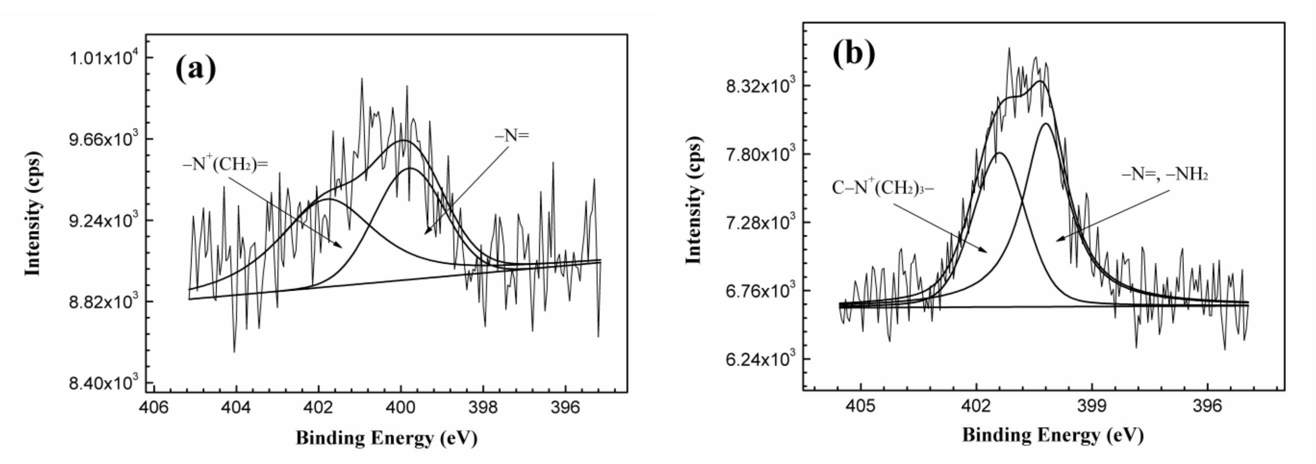

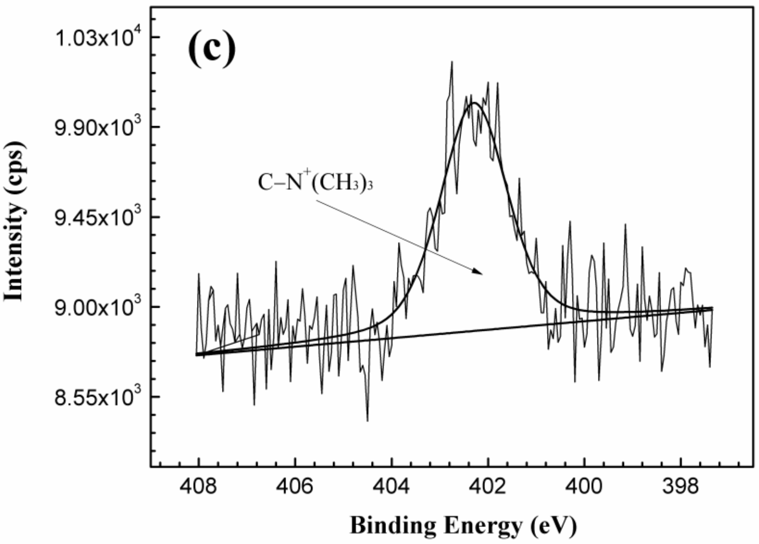

Figure 10. High-resolution XPS spectra of N_{1s} of Q235 steels pre-corroded for 3 days after the immersion in the CO_2/H_2S-saturated brine solution with (a) 50 mg L^{-1} BPC, (b) 50 mg L^{-1} IAS, and (c) 50 mg L^{-1} TTAB for 4 h at 60 ˚C.

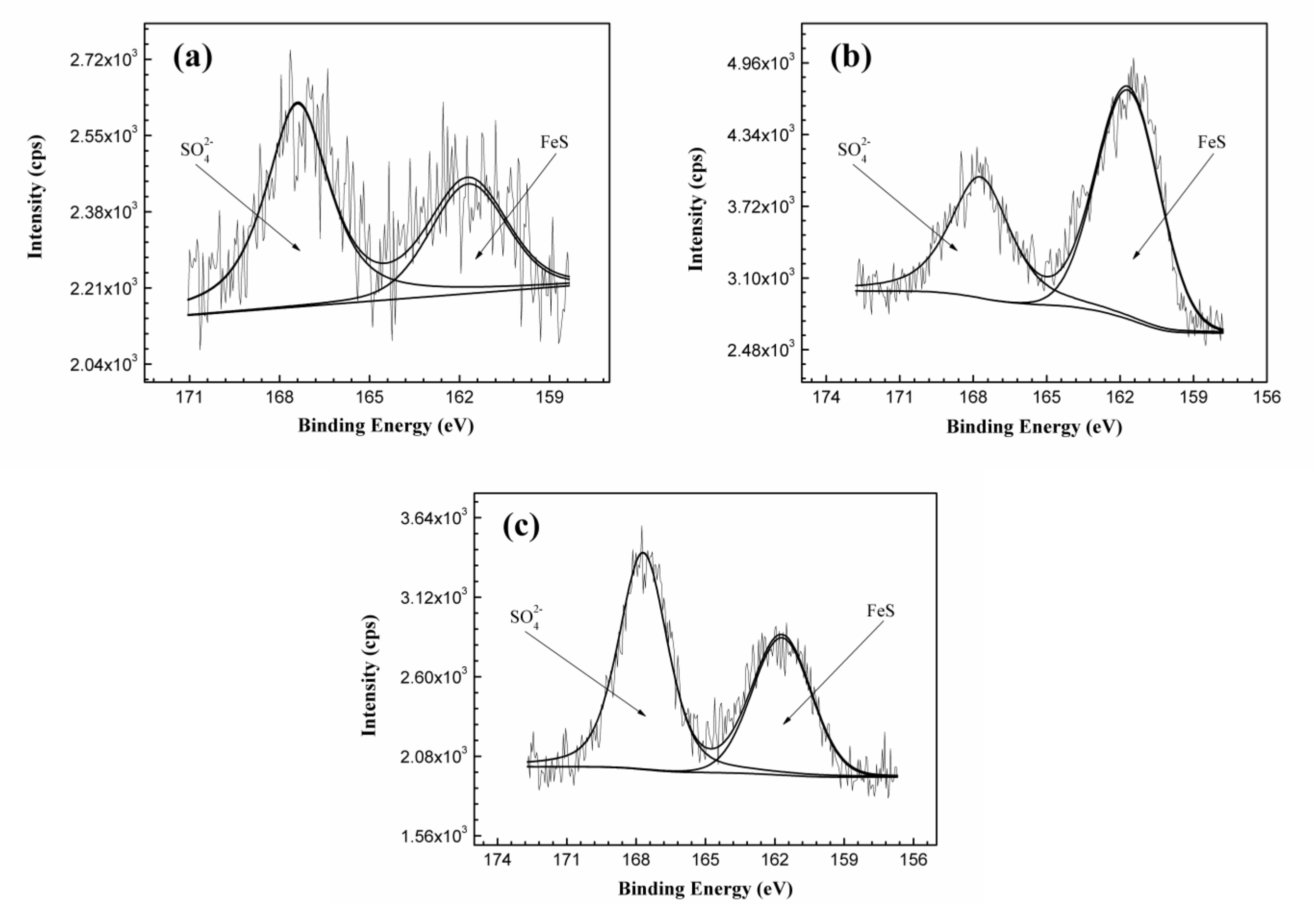

Figure 11. High-resolution XPS spectra of S_{2p} of Q235 steels pre-corroded for 3 days after the immersion in the CO_2/H_2S saturated brine solution with (a) 50 mg L^{-1} BPC, (b) 50 mg L^{-1} IAS, and (c) 50 mg L^{-1} TTAB for 4 h at 60 ˚C.

3.5 Discussion

In the CO_2/H_2S coexistent brine solution, the corrosion of steel was influenced by several factors, such as CO_2 partial pressure, H_2S partial pressure, temperature and pH of the solution [37, 38]. With the increase of the H_2S partial pressure, the corrosion of steel could be switched from CO_2 corrosion to H_2S corrosion [37, 39]. According to the different environments, various types of corrosion products of iron sulfide could be formed. Mackinawite is a sulfur-deficient iron sulfide with a tetragonal unit cell [40], and is mainly formed on the steel surface in saturated CO_2/H_2S solution [37], which has been proved with the XRD results in this study. In some cases, the corrosion product of iron sulfide can effectively prevent the corrosive medium from diffusing to the steel matrix, thus to decrease the corrosion rate of steel [37, 41]. This phenomenon was observed in this study according to the potentiodynamic polarization measurements (the corrosion current density was decreased significantly with the increase of pre-corrosion time due to the formation of corrosion products mainly containing FeS).

According to the theory of Lewis acid-base, the corrosion inhibitors, such as BPC, IAS and TTAB, were Lewis bases, and the metallic substrate would act as Lewis acid. The protection action of inhibitors could be attributed to the Lewis acid-base interaction between the inhibitor molecules and metallic substrate [42]. Therefore, a compact inhibitor film can be formed on the surface of the freshly abraded steels resulting in good corrosion inhibition performance of the inhibitors.

When the steel was pre-corroded for a short time (like 4 hours and 1 day), the steel matrix was incompletely covered by some corrosion products according to XRD results, and Fig. 7(a) indicates that the corrosion product layer is very thin. Compared with metallic iron, the inhibitors would be more strongly adsorbed on the external corrosion products of $FeCO_3$ and FeS through Lewis acid-base interactions [43]. Therefore, the inhibitors could be adsorbed on the surfaces of steel matrix and corrosion products, simultaneously, to inhibit the CO_2/H_2S corrosion of the pre-corroded steel (Fig. 12(a)). However, the porous corrosion product film could also provide some diffusion channels for corrosion species leading to the attack of steel matrix below the corrosion product film, which finally resulted in the deterioration of the performance of inhibitors.

When the pre-corrosion time was relative long (like 3 to 7 days), the steel matrix was nearly covered by corrosion products. The inhibitor molecules, which were detected by XPS, might mainly be adsorbed on the surface of corrosion products (Fig. 12(b)). Therefore, the corrosion of steel could be retarded to some extent. However, a porous corrosion product film could be clearly observed in Fig. 7(b) or (c) on this case. The diffusion channels for corrosion species became more abundant with extended pre-corrosion time resulting in a more serious attack of the inner steel matrix. Therefore, the inhibition performance of inhibitors was deteriorated gradually with the increase of pre-corrosion time.

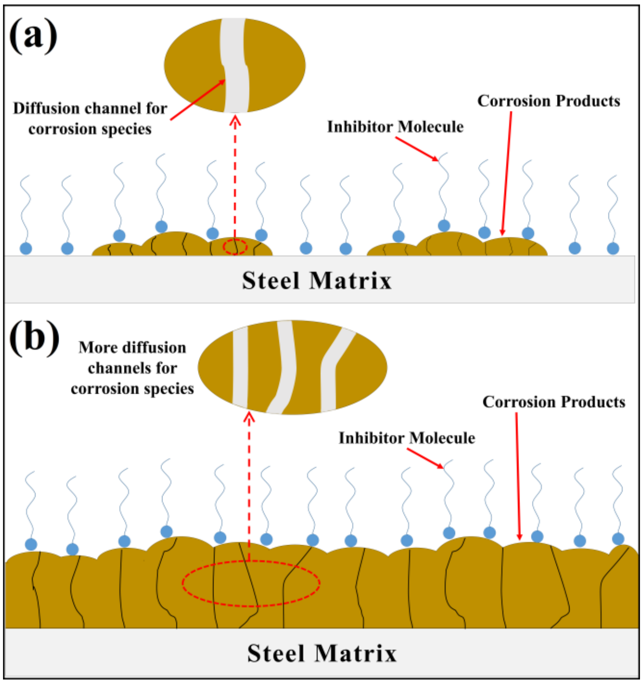

Figure 12. Sketches of possible adsorption behavior of inhibitors on the surface of samples pre-corroded for (a) short time and (b) long time in the CO_2/H_2S-saturated brine solution.

4. CONCLUSIONS

(1) The corrosion of Q235 steel in the CO_2/H_2S-saturated brine solution at 60 °C was mainly induced by H_2S corrosion, and the corrosion products were consist of mostly FeS and limited $FeCO_3$.

(2) According to electrochemical measurements, corrosion rate of the pre-corroded Q235 steel was significantly decreased with the increase of pre-corrosion time indicating the protection effect of corrosion products on steel matrix.

(3) Inhibitors of BPC, IAS and TTAB all had good corrosion inhibition effects on the freshly abraded Q235 steel in the CO_2/H_2S-saturated brine solution.

(4) Inhibitors could be adsorbed on the surface of the corrosion products and retard the CO_2/H_2S corrosion of the pre-corroded Q235 steel to some extent.

(5) A relative distinct difference of the performance of inhibitors could be observed after pre-corrosion for 7 days possibly due to the differences of their molecular structures.

(6) The corrosion inhibition performance of inhibitors was gradually deteriorated with the increase of pre-corrosion time possibly because the corrosion species could also diffuse through the diffusion channels to attack the steel matrix.

ACKNOWLEDGEMENT
The authors thank National Natural Science Foundation of China for the financial supports on this project (No. 51471021).

References

1. P. Rajeev, A. O. Surendranathan and C. S. N. Murthy, *J. Mater. Environ. Sci.,* 3 (2012) 856.
2. G. Fierro, G. M. Ingo and F. Mancia, *Corrosion*, 45 (1989) 814.
3. K. Masamura, S. Hashizume, J. Sakai and I. Matsushima, *Corrosion*, 43 (1987) 359.
4. S. Muralidharan, K. L. N. Phani, S. Pitchumani, S. Ravichandran and S. V. K. lyer, *J. Electrochem. Soc.*, 142 (1995) 1478.
5. F. Bentiss, M. Traisnel, N. Chaibi, B. Mernari, H. Vezin and M. Lagrenée, *Corros. Sci.*, 44 (2002) 2271.
6. D. Chebabe, Z. A. Chikh, N. Hajjaji, A. Srhiri and F. Zucchi, *Corros. Sci.,* 45 (2003) 309.
7. C. Zhang, H. Duan and J. Zhao, *Corros. Sci.,* 112 (2016) 160.
8. M. Elachouri, M. S. Hajji, S. Kertit, E. M. Essassi, M. Salem and R. Coudert, *Corros. Sci.*, 37 (1995) 381.
9. G. Schmitt, *Brit. Corros. J.*, 19 (1984) 165.
10. B. Mernari, H. El Attari, M. Traisnel, F. Bentiss and M. Lagrenee, *Corros. Sci.*, 40 (1998) 391.
11. I. B. Obot, D. D. Macdonald and Z. M. Gasem, *Corros. Sci.*, 99 (2015) 1.
12. O. Benali, L. Larabi, M. Traisnel, L. Gengembre and Y. Harek, *Appl. Surf. Sci.*, 253 (2007) 6130.
13. Z. A. Iofa and V. V. Batrakov, *Electrochim. Acta*, 9 (1964) 1645.
14. P. C. Okafor and Y. Zheng, *Corros. Sci.*, 51 (2009) 850.
15. J. Zhao, H. Duan and R. Jiang, *Corros. Sci.*, 91 (2015) 108.
16. R. Nyborg, E. Gulbrandsen, T. Løland and K. Nisancioglu, Effect of steel microstructure and composition on inhibition of CO_2 corrosion, NACE International, Orlando, Florida, USA, 2000, paper no. 23.
17. E. Gulbrandsen, S. Nesic, A. Stangeland and T. Burchardt, Effect of precorrosion on the performance of inhibitors for CO_2 corrosion of carbon steel, NACE International, San Diego, California, USA, 1998, paper no. 13.
18. H. Zhang, X. Pang, M. Zhou, C. Liu, L. Wei and K. Gao, *Appl. Surf. Sci.*, 356 (2015) 63.
19. S. D. Kapusta, P. R. Rhodes and S. A. Silverman, Inhibitor testing for CO_2 environmrnts, NACE International, Houston, Texas, USA, 1991, paper no. 471.
20. L. D. Paolinelli, T. Pérez and S. N. Simison, *Corros. Sci.*, 50 (2008) 2456.
21. R. H. Hausler and D. W. Stegman, Laboratory studies on flow induced localized corrosion in CO_2/H_2S exironments, IV. Assessment of the Kinetics of corrosion inhibition by hydrogen evolution measurements, NACE International, Houston, Texas, USA, 1991, paper no. 474.
22. R. H. Hausler, D. W. Stegman, C. I. Cruz and D. Tjandroso, Laboratory studies on flow induced localized corrosion in CO_2/H_2S exironments, III. Chemical corrosion inhibition, NACE International, Houston, Texas, USA, 1990, paper no. 7.
23. H. Malik, *Corrosion*, 51 (1995) 321.
24. A. Singh, Y. Lin, I. B. Obot and E. E. Ebenso, *J. Mol. Liq.*, 219 (2016) 865.
25. E. S. Ferreira, C. Giacomelli, F. C. Giacomelli and A. Spinelli, *Mater. Chem. Phys.*, 83 (2004) 129.
26. A. V. Benedeti, P. T. A. Sumodjo, K. Nobe, P. L. Cabot and W. G. Proud, *Electrochim. Acta*, 40 (1995) 2657.
27. M. V. Azghandi, A. Davoodi, G. A. Farzi and A. Kosari, *Corros. Sci.*, 64 (2012) 44.
28. S. Delpeux, F. Beguin, R. Benoit, R. Erre, N. Manolova and I. Rashkov, *Eur. Polym. J.*, 34 (1998) 905.
29. W. Meyer, M. Grunze, R. Lamb, A. Ortega-Vilamil, W. Schrepp and W. Braun, *Surf. Sci.*, 273 (1992) 205.
30. O. Olivares-Xometl, N. V. Likhanova, M. A. Domínguez-Aguilar, J. M. Hallen, L. S. Zamudio and E. Arce, *Appl. Surf. Sci.*, 252 (2006) 2139.
31. J. M. Bonello and R. M. Lambert, *Surf. Sci.*, 498 (2002) 212.
32. Z. J. Yu, E. T. Kang and K. G. Neoh, *Polymer*, 43 (2002) 4137.

33. J. Xu, X. Han, H. Liu and Y. Hu, *Colloid. Surface*. A, 273 (2006) 179.
34. S. Nakamura and A. Yamamoto, *Sol. Energ. Mat. Sol*. C, 65 (2001) 79.
35. B. C. Bostick and S. Fendorf, *Geochim. Cosmochim*. Ac, 67 (2003) 909.
36. R. V. Kashkovskiy, Y. I. Kuznetsov and L. P. Kazansky, *Corros. Sci*., 64 (2012) 126.
37. Z. F. Yin, W. Z. Zhao, Z. Q. Bai, Y. R. Feng and W. J. Zhou, *Electrochim. Acta*, 53 (2008) 3690.
38. Y. S. Choi, S. Nesic and S. Ling, *Electrochim. Acta*, 56 (2011) 1752.
39. C. Ren, D. Liu, Z. Bai and T. Li, *Mater. Chem. Phys*., 93 (2005) 305.
40. J. S. Smith and J. D. A. Miller, *Brit. Corros. J*., 10 (1975) 136.
41. T. Murata, R. Matsuhashi, T. Taniguchi and K. Yamamoto, The evaluation of H_2S containing environments from the viewpoint of OCTG and linepipe for sour gas applications, Offshore Technology Conference, Houston, Texas, USA, 1979, 1307.
42. S. Martinez, *Mater. Chem. Phys*., 77 (2003) 97.
43. D. A. Lopez, S. N. Simison and S. R. De Sanchez, *Corros. Sci*., 47 (2005) 735.